Eur J Nucl Med Mol Imaging (2009) 36:2058–2067
DOI 10.1007/s00259-009-1220-z

ORIGINAL ARTICLE

^{68}Ga-DOTA-RGD peptide: biodistribution and binding into atherosclerotic plaques in mice

Johanna Haukkala · Iina Laitinen · Pauliina Luoto · Peter Iveson · Ian Wilson · Hege Karlsen · Alan Cuthbertson · Jukka Laine · Pia Leppänen · Seppo Ylä-Herttula · Juhani Knuuti · Anne Roivainen

Received: 8 April 2009 / Accepted: 1 July 2009 / Published online: 23 July 2009

Abstract
Purpose Increased expression of αvβ3/αvβ5 integrin is involved in angiogenesis and the inflammatory process in atherosclerotic plaques. The novel ^{68}Ga-DOTA-RGD peptide binds with high affinity to αvβ3/αvβ5 integrin. The aim of this study was to investigate the uptake of the ^{68}Ga-DOTA-RGD peptide in atherosclerotic plaques.
Methods Uptake of intravenously administered ^{68}Ga-DOTA-RGD peptide was studied ex vivo in excised tissue samples and aortic sections of LDLR$^{-/-}$ApoB$^{100/100}$ atherosclerotic mice. The uptake of the tracer in aortic cryosections was examined by using digital autoradiography. Subsequently, the autoradiographs were combined with histological and immunohistological analysis of the sections.
Results DOTA-RGD peptide was successfully labelled with the generator-produced ^{68}Ga. The tracer had reasonably good specific radioactivity (8.7±1.1 GBq/μmol) and was quite stable in vivo. According to ex vivo biodistribution results, ^{68}Ga-DOTA-RGD was cleared rapidly from the blood circulation and excreted through the kidneys to the urine with high radioactivity in the intestine, lungs, spleen and liver. Autoradiography results showed significantly higher uptake of ^{68}Ga-DOTA-RGD peptide in the atherosclerotic plaques compared to healthy vessel wall (mean ratio ± SD 1.4±0.1, p=0.0004).
Conclusion We observed that ^{68}Ga-DOTA-RGD is accumulated into the plaques of atherosclerotic mice. However, this data only shows the feasibility of the approach, while the clinical significance still remains to be proven. Further studies are warranted to assess the uptake of this tracer into human atherosclerotic plaques.

Keywords Atherosclerosis · Plaque · ^{68}Ga · αvβ3/αvβ5 integrin · RGD · PET

J. Haukkala · I. Laitinen · P. Luoto · J. Knuuti · A. Roivainen (✉)
Turku PET Centre, University of Turku,
Kiinamyllynkatu 4-8,
FI-20520 Turku, Finland
e-mail: anne.roivainen@utu.fi

P. Iveson · I. Wilson
GE Healthcare Biosciences, Medical Diagnostics,
London, UK

H. Karlsen · A. Cuthbertson
GE Healthcare MDx Research,
Nycovein 2,
Oslo, Norway

J. Laine
Department of Pathology, Turku University Hospital,
Turku, Finland

P. Leppänen · S. Ylä-Herttula
A.I. Virtanen Institute, University of Kuopio,
Kuopio, Finland

A. Roivainen
Turku Centre for Disease Modelling, University of Turku,
Turku, Finland

Introduction

Inflammation has a prominent role in atherosclerosis, and may persist for several years before the appearance of clinical manifestations. A stable atherosclerotic plaque usually contains a small lipid core covered by a thick fibromuscular cap, while an unstable plaque is often composed of a large lipid core, a thin cap and a larger amount of inflammatory cells, mostly macrophages. Rupture of an unstable vulnerable plaque is the main cause of acute coronary syndrome and myocardial infarction. Identification of plaques vulnerable to rupture could possibly guide the local therapy and prevent clinical complications [1–3].

At present, there are no reliable methods for identifying atherosclerotic plaques in vivo. Several invasive and non-invasive diagnostic methods are currently under development or being tested for facilitating the detection of vulnerable plaques by using, for example, X-ray computed tomography angiography (CTA) [4], magnetic resonance imaging (MRI) [5], optical coherence tomography (OCT) [6] or intravascular ultrasound (IVUS) [7]. None of these techniques have proven their value in extensive in vivo validation studies, although they have been able to delineate certain features of plaques. Other drawbacks include the lack of prospective data and/or insufficient resolution [7]. Markers of inflammation and tissue remodelling within plaques would probably be ideal indicators of vulnerability. The most commonly tested tracer for the inflammatory process in plaques is 2-[^{18}F]fluoro-2-deoxy-D-glucose ([^{18}F]FDG). However, [^{18}F]FDG is not a specific tracer for inflammation, but is also avidly accumulated in activated muscle and cancerous tissues, and also in the calcified structures of the vessel wall [8].

Atherosclerotic lesions responsible for vascular occlusions are associated with angiogenesis within the vessel wall. Plaque neovascularisation is comprised of a network of capillaries that arise from the adventitial vasa vasorum and extend into the intimal layer of atherosclerotic lesions. As to their function, these plaque capillaries are proposed as important regulators of plaque growth and lesion instability. Microvessels in the intima are immature, which may result in intraplaque haemorrhage. Increased density of microvessels is associated with intraplaque haemorrhage and plaque rupture [9, 10].

The αvβ3 and αvβ5 integrins are transmembrane glycoproteins that are involved in the migration of activated endothelial cells during the formation of new vessels. In atherosclerotic plaques, αvβ3 integrin is expressed in endothelial cells, medial and some intimal smooth muscle cells (SMCs) [11]. Expression of αvβ3 integrin is found in the shoulder of advanced plaques and in the necrotic core of human atherosclerotic lesions. CD68-positive macrophages also strongly express αvβ3 integrin [12]. In addition to αvβ3 integrin, αvβ5 is also expressed in the intima of human atherosclerotic plaques [13]. However, for in vivo imaging purposes, the integrin αvβ3 is the most extensively examined marker of angiogenesis [14].

The development of radiolabelled ligands for the αvβ3/αvβ5 integrin might facilitate the imaging of atherosclerotic plaques [15]. For the present study, we explored the feasibility of a novel ^{68}Ga-labelled monomeric, 1,4,7,10-tetraazacyclododecane-N',N'',N''',N''''-tetraacetic acid conjugated ^{68}Ga-DOTA-RGD peptide (Fig. 1) binding to the αvβ3/αvβ5 integrin in the assessment of the degree of inflammation and the vulnerability of atherosclerotic plaques. The biodistribution of the radiopeptide and uptake to plaques were evaluated in atherosclerotic LDLR$^{-/-}$ApoB$^{100/100}$ mice by measuring the radioactivity of excised organs and using digital autoradiography of aortic cryosections.

Materials and methods

Radiotracer synthesis

DOTA-RGD peptide was obtained from GE Healthcare (Oslo, Norway). The synthesis of DOTA-RGD peptide has been described by Indrevoll et al. The in vitro affinity of the DOTA-RGD peptide for αvβ3/αvβ5 integrin is 3.2 nM [16]. DOTA-RGD peptide was labelled with ^{68}Ga obtained in the form of $^{68}GaCl_3$ from a ^{68}Ge/^{68}Ga generator (Cyclotron Co., Obninsk, Russia) by elution with 0.1 M HCl. The elution of the ^{68}Ge/^{68}Ga generator was monitored on-line with a positron-sensitive photodiode detector (Hamamatsu S5591, Hamamatsu Photonics K.K. Solid State Division, Japan). The nominal ^{68}Ge activity loaded onto the generator column was 1,850 MBq (50 mCi). The radioactive elution peak was collected for the ^{68}Ga-labeling of DOTA-RGD peptide. The $^{68}GaCl_3$ eluate (0.5 ml) was mixed with 4-(2-hydroxyethyl)-1-piperazineethanesulfonic acid (120 mg; $C_8H_{18}N_2O_4S$, M (HEPES) = 238.3 g/mol, Sigma-Aldrich Chemie, Germany) to give a pH of approximately 4.4. Next, DOTA-RGD peptide (13 μl/1 mM, 13 nmol, 21.4 μg) was added and the mixture was incubated at 100°C for 20 min. No further purification was needed. The radiochemical purity was determined by reversed-phase radio-HPLC (μBondapak C18, 7.8×300 mm, 125 Å, 10 μm; Waters, Milford, MA). The HPLC conditions for ^{68}Ga-DOTA-RGD peptide were as follows: flow 5 ml/min, A=2.5 mM trifluoroacetic acid (TFA), B = acetonitrile (MeCN), C=50 mM phosphoric acid. Linear A/B/C gradient: 0–2 min 100/0/0, 2–10 min from 100/0/0 to 35/65/0, 10–11 min from 0/35/65 to 0/0/100, 11–18 min 0/0/100, λ=218 nm. The compounds in the samples were separated by comparing the retention times of unlabelled peptide and authentic standards ^{68}Ga-DOTA and $^{68}Ga^{3+}$. The radio-HPLC system consisted of LaChrom instruments (Hitachi; Merck, Darmstadt, Germany) including pump L7100, UV detector L-7400 and interface D-7000; an on-line radioactivity detector (Radiomatic 150 TR, Packard, Meriden, CT); and a computerized data acquisition system.

Animals

Six male mice deficient of LDL receptor and expressing only apolipoprotein B100 (LDLR$^{-/-}$ApoB$^{100/100}$, Jackson Laboratory, Bar Harbor, ME, strain #003000) were used. The LDLR$^{-/-}$ApoB$^{100/100}$ double-knockout mouse model is described by Heinonen et al. They showed that this mouse model develops atherosclerotic plaques in the arteries and that their plasma cholesterol level is highly increased

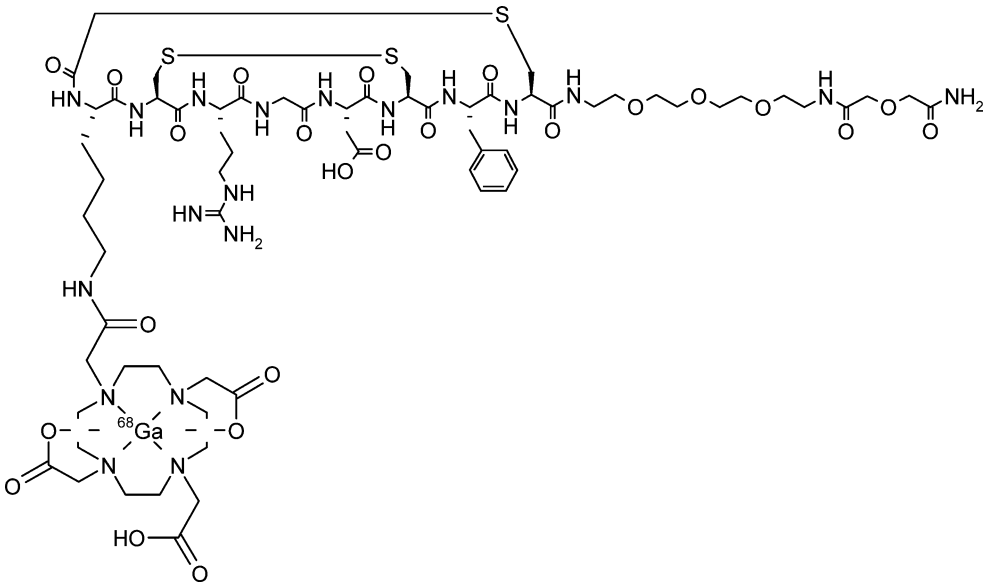

Fig. 1 Schematic structure of ^{68}Ga-labelled DOTA-RGD peptide (molecular weight= 1,645 g/mol). ^{68}Ga is attached to the DOTA chelator

already 3 months after a lipid-rich diet [17]. In the present study, the mice were kept on a high-fat, Western-type diet (TD 88137, Harlan Teklad, with 42% of calories coming from fat and 0.2% from cholesterol, without sodium cholate) for 5 months, starting at the age of 6–7 months. Six male C57BL/6 J Bom strain mice fed with a regular chow diet served as non-atherosclerotic controls. The age and weight were 11.5±0.5 months and 39±6 g (mean ± SD) for the LDLR$^{-/-}$ApoB$^{100/100}$ mice, and 14±0 months and 41±4 g for the C57BL/6 J Bom control mice. All mice were housed throughout the study in an animal facility under standard conditions with lights on from 6.00 a.m. to 6.00 p.m. and with ad libitum access to water and food. The experiments were approved by the Laboratory Animal Care and Use Committee of the University of Turku, Finland.

In vivo stability of ^{68}Ga-DOTA-RGD peptide

To examine the stability of ^{68}Ga-DOTA-RGD peptide, a blood sample (0.8 ml) obtained through a cardiac puncture (six LDLR$^{-/-}$ApoB$^{100/100}$ mice, six control mice) and a urine sample (five LDLR$^{-/-}$ApoB$^{100/100}$ mice, two control mice) were collected 60 min after intravenous injection. The plasma was separated by centrifugation (2,118 × *g* for 5 min) at +4°C. Proteins of plasma and urine were precipitated using 10% sulfosalisylic acid. A supernatant obtained after centrifugation followed by filtration through syringe filter (0.45 μm, Waters Corporation, USA) was analysed by radio-HPLC as described above.

Ex vivo distribution of ^{68}Ga-DOTA-RGD in atherosclerotic and control mice

^{68}Ga-DOTA-RGD peptide (17±4 MBq, 3.0±0.5 μg) was administrated intravenously via a tail vein in non-anaesthetised mice (six LDLR$^{-/-}$ApoB$^{100/100}$ mice and six C57BL/6 J Bom mice). At 60 min after injection, blood samples were drawn under deep isoflurane anaesthesia into heparinised tubes by cardiac puncture, and thereafter the mice were sacrificed with cervical dislocation. Samples of blood and various tissues were collected, patted dry and weighted, and the radioactivity was measured using an automatic gamma counter (1480 Wizard 3" Gamma Counter; EG & G Wallac, Turku, Finland) cross-calibrated with a dose calibrator (VDC-202, Veenstra Instruments, Joure, The Netherlands). Background counts were subtracted, and the radioactivity decay was corrected to the time of injection. The dose remaining in the tail was also compensated. The radioactivity concentration that had accumulated in the tissue samples over the 60-min period following the ^{68}Ga-DOTA-RGD injection was expressed as a percentage of the injected dose per gram of tissue (%ID/g).

Autoradiographic analysis of aortic cryosections

The distribution of ^{68}Ga-DOTA-RGD peptide to aorta tissue was studied with digital autoradiography in six LDLR$^{-/-}$ApoB$^{100/100}$ mice and six control mice. The aorta, from ascending aorta to the level of diaphragm, was dissected and blood was removed with saline. The aorta and an internal control muscle sample from the same animal were frozen, and sequential longitudinal 8- and 20-μm sections were cut with a cryomicrotome at –15°C and thaw-mounted onto microscope slides. The sections were air dried for 5 min and apposed to an imaging plate (Fuji Imaging Plate BAS-TR2025, Fuji Photo Film Co., Ltd., Japan). After an exposure time of 2.5 h, the imaging plates were scanned with Fuji Analyser BAS-5000 (Fuji Tokyo, Japan; internal resolution 25 μm). The autoradiographs were analysed for count densities (photostimulated

luminescence per unit area, PSL/mm^2) with an analysis programme (Tina 2.1, Raytest Isotopemessgeräte, GmbH, Straubenhardt, Germany). Four types of regions of interest (ROIs) were drawn according to the histology, and the background area count densities were subtracted from the image data. The ROIs were analysed from (1) plaque, (2) adventitia, (3) healthy vessel wall, and (4) muscle (internal control). The radioactivity uptake values were normalized against the control site (muscle).

Reliability of ARG method

Autoradiography (ARG) analyses were performed by two independent observers. Reproducibility of the autoradiography results was evaluated by calculating the coefficient of variation (CV%), mean difference and intra-class factor. A CV of ≤10% is considered acceptable. The average of various ROIs was calculated for each animal from the other observer's analyses.

Histology and immunohistochemical staining

After autoradiography, the 20-μm sections were stained with haematoxylin and eosin (HE) and studied for morphology under a light microscope. The degree of inflammation was semi-quantitatively assessed as the number of macrophages and other leukocytes in the tissue. Adjacent sections were immunostained with anti-CD31 antibody (endothelial marker) and parallel sections with Mac-3 antibody (mouse macrophages). For the staining of CD31 in mouse aorta, the sections were stored at –70°C, melted, fixed 10 min in ice-cold acetone and air dried. Endogenous peroxidase was blocked (DakoCytomation, S2001, Denmark). The sections were incubated for 1 h with primary rat anti-mouse CD31 antibody (AB Serotec, MCA1364, Clone 390, Oxford UK; working dilution 1:400 with 3% BSA) and for 30 min with secondary biotinylated mouse anti-rat antibody (BD Pharmingen, BD550325, USA; working dilution 1:100 with 0.05 M Tris-HCl, pH 7.6 + 0.05% Tween 20). For Mac-3 staining, 8-μm sections were stored at –70°C, melted and fixed for 10 min in 4% formaldehyde (pH 7.0). Mac-3 antigen was uncovered by boiling in hot 10 mM citrate buffer (pH 6.0) for 20 min. Then the sections were incubated for 1 h with primary rat anti-mouse Mac-3 antibody (BD Pharmigen, BD550292, Clone M3/84, USA; working dilution 1:5000 with 3% BSA), and endogenous peroxidase was blocked with 1% hydrogen peroxide. Thereafter, the sections were incubated for 30 min with polyclonal rabbit anti-rat antibody (Dako, E0468, Denmark; working dilution 1:200 with 0.05 M Tris-HCl, pH 7.6 + 0.05% Tween 20) and for 30 min with tertiary EnVision+ System- HRP-labelled goat anti-rabbit antibody (DakoCytomation, K4003, Denmark; working dilution 1:200 with 0.05 M Tris-HCl, pH 7.6 + 0.05% Tween 20). Finally, Mayer's haematoxylin was used for counterstaining.

Estimation of degree of inflammation

The degree of inflammation in the plaques was semi-quantitatively assessed by the first author together with an experienced pathologist (J.L.). In the semi-quantitative analysis of Mac-3 stained areas, the plaques were divided as non-inflamed (= no or occasional Mac-3 stained leucocytes) or inflamed (= moderate or severe inflammation categories present) as described in Laitinen et al.[8]. ROI analysis was made from parallel sections of Mac-3 antibody stained sections, and areas in the plaques were defined, according to the histology, as belonging to one or the other category. Only the endothelia of healthy vessel wall and plaque were stained with anti-CD31-antibody. There were no anti-CD31-stained regions inside the plaques.

Statistical methods

All results are expressed as mean ± SD values. *T*-test and one-way ANOVA were used to examine the significance of differences observed in ex vivo biodistribution study between the atherosclerotic LDLR$^{-/-}$ApoB$^{100/100}$ mice and the control mice. *T*-test with a mixed Dunnett's model was applied to correct *p*-values of the biodistribution of aortic uptake versus different tissue uptakes in the atherosclerotic and control-mice groups. In autoradiography analysis, a mixed model with Tukey-Kramer corrected *p*-values was applied to individual mean values of ROIs. A value of *p* less than 0.05 was considered to be statistically significant.

Results

Radiolabelling

The radiochemical purity of ^{68}Ga-DOTA-RGD peptide was 97±2% (n=8) as analysed by radio-HPLC. The specific radioactivity of the reaction mixture was 8.7±1.1 GBq/μmol. Under the conditions described above, the retention time of ^{68}Ga-DOTA-RGD peptide was 8.08±0.11 min (Fig. 2a). The entire labelling procedure, including the radio-HPLC analysis and elution of ^{68}Ga, was completed within 40 min.

In vivo stability of ^{68}Ga-DOTA-RGD peptide

The radio-HPLC analysis of the mouse-plasma samples from LDLR$^{-/-}$ApoB$^{100/100}$ mice (n=6) and control mice (n=6) showed 70.3±5.2% and 65.9±5.2% of unchanged ^{68}Ga-DOTA-RGD peptide, respectively, at 1 h after injection. In

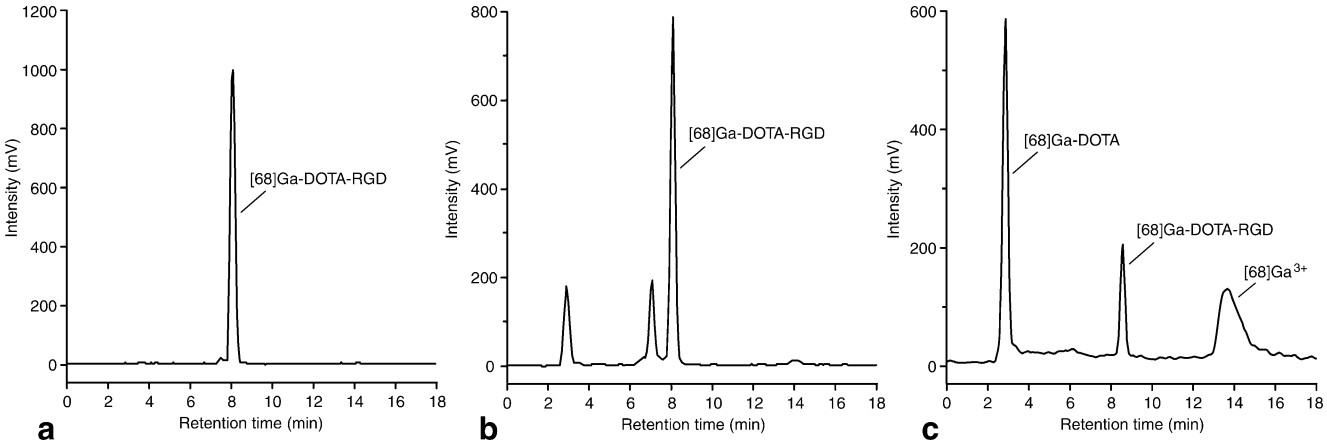

Fig. 2 Representative radio-HPLC chromatograms of **a** intact ^{68}Ga-DOTA-RGD peptide, **b** mouse (LDLR$^{-/-}$/ApoB$^{100/100}$) plasma obtained 1 h after intravenous injection of ^{68}Ga-DOTA-RGD peptide, and **c** a mixture of authentic standards

the urine, the percentages of unchanged peptide were 3.3±1.0% for LDLR$^{-/-}$ApoB$^{100/100}$ mice (n=5) and 2.8±1.0% for control mice (n=2) at 1 h after injection.

No degradation products of ^{68}Ga-DOTA-RGD peptide were identified. According to the radio-HPLC analysis, the retention times of degradation products were 2.90±0.10 min, 7.09±0.14 min, and 13.86±0.09 min, representing 15.0±8.4%, 14.0±7.0%, and 1.3±0.7% of total radioactivity, respectively. A representative radio-HPLC chromatogram of the mouse-plasma sample is shown in Fig. 2b. For comparison, the retention times of authentic standards ^{68}Ga-DOTA and ^{68}Ga^{3+} were 2.89±0.03 min and 13.59±0.11 min (Fig. 2c), respectively.

Characterisation of atherosclerosis in LDLR$^{-/-}$ApoB$^{100/100}$ and control mice

After 5 months on a Western-type diet, the LDLR$^{-/-}$ApoB$^{100/100}$ mice had large areas of aorta covered in plaques, also in the distal part of the aorta. Plaques were found in the proximal parts of brachiocephalic, subclavia and carotic arteries and in the pulmonary artery. The plaques were of fibroatheroma type and some contained calcifications. Leukocyte infiltration was observed in plaques in all LDLR$^{-/-}$ApoB$^{100/100}$ mice, and based on the histological analysis, the inflammation was estimated to be of moderate degree (occasional polymorphonuclear leukocytes or lymphocytes and some groups of inflammatory cells). Mac-3 staining revealed areas in the plaques with a moderate number of macrophages (Fig. 3). The anti-CD31 antibody stained the endothelia of the vessel wall and plaque (Fig. 4). No atherosclerosis was detected in the aortas of the control mice. The mice in the control group were approximately of the same age (14 months vs. 11.5 months) and weight (41 g vs. 39 g) as the LDLR$^{-/-}$ApoB$^{100/100}$ mice, and both groups included only male mice.

Ex vivo biodistribution of ^{68}Ga-DOTA-RGD

The uptake of ^{68}Ga-DOTA-RGD in different tissues is shown in Table 1. The highest level of ^{68}Ga-DOTA-RGD uptake was found in the kidneys in LDLR$^{-/-}$ApoB$^{100/100}$ mice (5.1±1.6%ID/g at 1 h) and in control mice (6.3±1.9% ID/g at 1 h). The levels of uptake in the liver (2.3±1.0%ID/g and 2.5±0.8%ID/g, respectively, at 1 h) and intestine (2.8±0.4%ID/g and 2.2±0.5%ID/g, respectively, at 1 h) were

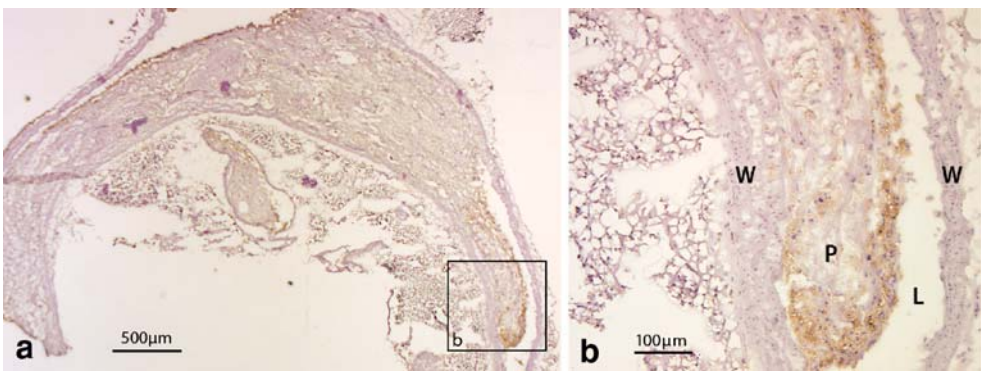

Fig. 3 **a** Macrophage (Mac-3)-stained aortic arch with enlarged macrophage positive plaque (**b**) (*brown colour in plaque*). Adventitia and healthy vessel wall are not stained with Mac-3 stain. *L* lumen, *P* plaque, *W* wall

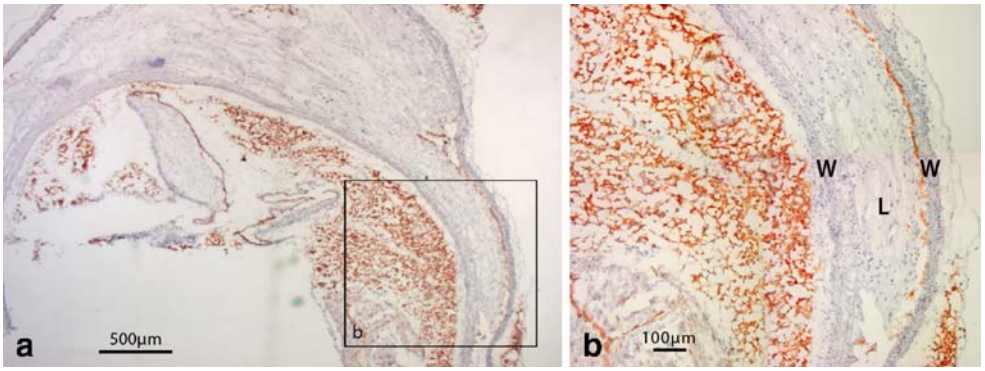

Fig. 4 **a** Anti-CD31 stains the endothelial cells (*red*) of the healthy vascular wall and on the surface of the plaques **b** enlarged picture. Adventitia shows high unspecific staining (control staining not shown). *L* lumen, *P* plaque, *W* wall

significantly lower ($p<0.05$) in comparison to the kidneys, indicating the predominance of the renal excretion route and minor hepatobiliary excretion in atherosclerotic and control mice. The aortic uptake and biodistribution of ^{68}Ga-DOTA-RGD was 0.90±0.21%ID/g in LDLR$^{-/-}$ApoB$^{100/100}$ mice and 0.70±0.20%ID/g in control mice (p=ns). The aorta samples contained large amounts of adventitial tissue, mainly fat, in both atherosclerotic and control mice. The aorta/heart and aorta/blood uptake ratios were 1.8 and 1.1, respectively, in LDLR$^{-/-}$ApoB$^{100/100}$ mice and 1.3 and 0.9, respectively, in control mice.

Digital autoradiography of aortic sections

Autoradiographs of 11–13 aortic sections from each LDLR$^{-/-}$ApoB$^{100/100}$ mouse (n=6) and 8–11 aortic sections from each control animal (n=6) were analysed. In total, 1,309 ROIs (414 plaque; 334 healthy vessel wall; 513 adventitia and 48 muscle) were analysed from 12 mice. For each mouse, the mean uptakes of ^{68}Ga-radioactivity in the healthy vessel wall, adventitia and plaque were calculated and normalized against the internal control (= muscle).

Autoradiography analysis revealed significantly higher uptakes of ^{68}Ga-radioactivity in plaques as compared to the healthy vessel wall and adventitia. The plaque/wall ratio was 1.4±0.1 (plaque vs. wall uptake p=0.0004) and the plaque/adventitia ratio was 1.6±0.1 (plaque vs. adventitia uptake p=0.0002) in LDLR$^{-/-}$ApoB$^{100/100}$ mice (Table 2; Fig. 5). The accumulation of ^{68}Ga-radioactivity in the adventitia as compared to the healthy wall was statistically significant in LDLR$^{-/-}$ApoB$^{100/100}$ mice (p=0.014) and in control mice (p=0.0026). In the control mice, the uptake in the vessel wall was 2.4±0.6-fold higher than in the muscle and in the adventitia 1.7±0.4-fold higher than in the muscle.

Estimation of degree of inflammation

The ^{68}Ga-radioactivity uptakes and the macrophage contents in the plaques were compared using 4-6 Mac-3-stained aortic sections of each mouse. In total, 152 ROIs were analysed; 72 non-inflamed plaque regions and 80 inflamed plaque regions from atherosclerotic mice autoradiographs. No difference was found in comparing ^{68}Ga-

Table 1 Ex vivo biodistribution of ^{68}Ga-DOTA-RGD peptide in LDLR/ApoB48 and control mice

	LDLR/ApoB48 (n=6)	Control (n=6, bladder n=5)	p-value
Aorta	0.91±0.21*	0.70±0.20	NS**
Bladder	2.54±0.40	2.19±0.82	NS
Blood	0.84±0.32	0.83±0.21	NS
Bone	0.90±0.36	0.88±0.19	NS
Fat	0.18±0.07	0.22±0.13	NS
Heart	0.51±0.14	0.53±0.12	NS
Intestine	2.84±0.40	2.19±0.55	0.04
Kidney	5.10±1.57	6.27±1.91	NS
Liver	2.30±1.00	2.52±0.80	NS
Lungs	2.27±0.57	2.16±0.22	NS
Lymph nodes	1.70±0.43	1.51±0.28	NS
Muscle	0.47±0.36	0.40±0.13	NS
Pancreas	0.57±0.12	0.46±0.12	NS
Spleen	1.95±0.51	1.94±0.23	NS
Thymus	1.01±0.31	0.91±0.10	NS

* %ID/g (mean ± SD)

** Difference between atherosclerotic and control mice

NS not significant

Table 2 Normalized autoradiography results. Uptake of ^{68}Ga-DOTA-RGD in regions of interest (ROI) for each atherosclerotic mouse

Animal ID	Plaque	Wall	Adventitia
1	4.3±0.8* (*n*=51) **	2.8±0.7 (*n*=15)	2.4±0.4 (*n*=48)
2	4.6±0.9 (*n*=52)	3.3±0.9 (*n*=20)	2.9±0.4 (*n*=56)
3	2.6±0.6 (*n*=86)	1.6±0.5 (*n*=25)	1.6±0.3 (*n*=62)
4	3.3±0.7 (*n*=68)	2.5±0.5 (*n*=24)	2.2±0.5 (*n*=54)
5	3.9±0.6 (*n*=77)	2.8±0.5 (*n*=21)	2.3±0.5 (*n*=57)
6	4.9±0.8 (*n*=80)	3.5±0.9 (*n*=28)	2.9±0.5 (*n*=71)
Mean	3.9	2.8	2.4
SD	0.9	0.7	0.5

* The intensity (PSL/mm^2, mean ± SD); ** Number of ROIs; *t-test*; plaque vs. wall 0.0004; plaque vs. adventitia 0.0002; wall vs. adventitia 0.003

DOTA-RGD uptake between non-inflamed and inflamed plaque regions (ratio 1.1±0.2, p=0.36).

Reliability of ARG method

The analysis of mouse aortic sections is challenging because of the small size of aorta and allocation of ROIs to the autoradiograph. We used contour pictures to draw the ROI areas after which the ROI template was superimposed to the original ARG image for analyses. An example of ROI analysis is shown in Fig. 6. Use of parallel sections from the same aorta enables us to determine the radioactivity uptake for the whole aorta from the different tissue compartments, thus facilitating an accurate measurement as possible. All autoradiographs were analysed by two independent observers. The CV% for the ROI analyses of adventitia, plaque, healthy vessel wall and muscle was 4.5% (range 3.5–5.8%). The mean differences between two analysers for plaque versus adventitia, plaque versus healthy vessel wall, and plaque versus muscle were statistically insignificant (p>0.05 for all). The corresponding intra-class factors ranged between 0.90–0.97 (p=ns).

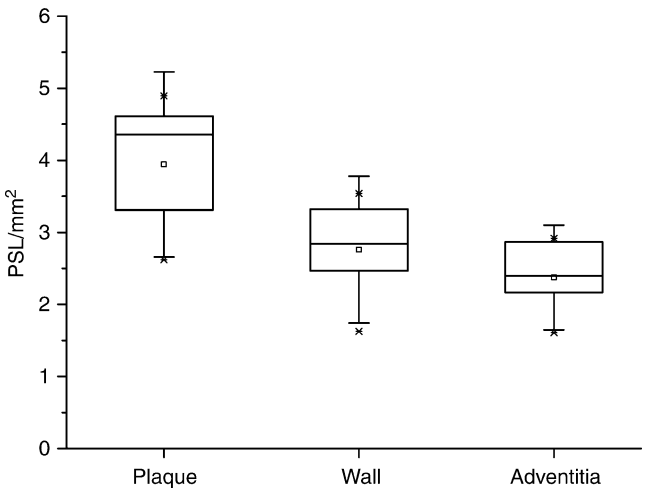

Fig. 5 Autoradiography analysis of normalized ^{68}Ga-DOTA-RGD peptide uptake in six LDLR$^{-/-}$/ApoB$^{100/100}$ mice

Discussion

Few imaging agents have been evaluated for PET imaging of atherosclerotic plaques in mice [8, 18]. Radiolabelled RGD peptides are of particular interest since they bind to αvβ3 integrin that is highly expressed in human atherosclerotic lesions [12]. The present study reports on the preclinical evaluation of a novel monomeric ^{68}Ga-DOTA-RGD peptide in the mouse model of atherosclerosis. Based on digital autoradiography of mouse aortic cryosections, our results revealed significantly higher uptakes of ^{68}Ga-DOTA-RGD peptide in the atherosclerotic plaques as compared to healthy vessel walls. Our results indicate the feasibility of the digital autoradiography approach, but the clinical meaning is, however, not yet conclusive.

^{68}Ga-labelled RGD peptides have been shown to have potential for the imaging of the angiogenesis and therapy of αvβ3 integrin-positive tumours [19–21]. To our knowledge, this is the first paper describing the use of ^{68}Ga-labelled RGD peptide for the purpose of imaging atherosclerotic plaques.

The αvβ3 and αvβ5 integrins are heterodimeric transmembrane glycoproteins, which are involved in the migration of activated endothelial cells during formation of new vessels. The αvβ3 and αvβ5 integrins are up-regulated in response to vascular damage and in certain types of tumours [22, 23]. Both αvβ3 and αvβ5 integrins are up-regulated in activated endothelial cells during angiogenesis, thus modulating cell survival and migration [24, 25]. Typically, enhanced expression of αvβ3 integrin is detected in the shoulder of advanced plaques and in the necrotic core of human atherosclerotic lesions [12]. Both αvβ3 and αvβ5 integrins are shown to be expressed in the human atherosclerotic intima [13] but, for in vivo imaging purposes, the αvβ3 is the most widely investigated marker of angiogenesis [14].

The in vitro affinity of the DOTA-RGD peptide used in this study has been evaluated for both αvβ3 and αvβ5 integrins, and is high enough for in vivo imaging [16]. The fact that the investigated ^{68}Ga-DOTA-RGD binds with both αvβ3 and αvβ5 integrins, can be an advantage for in vivo

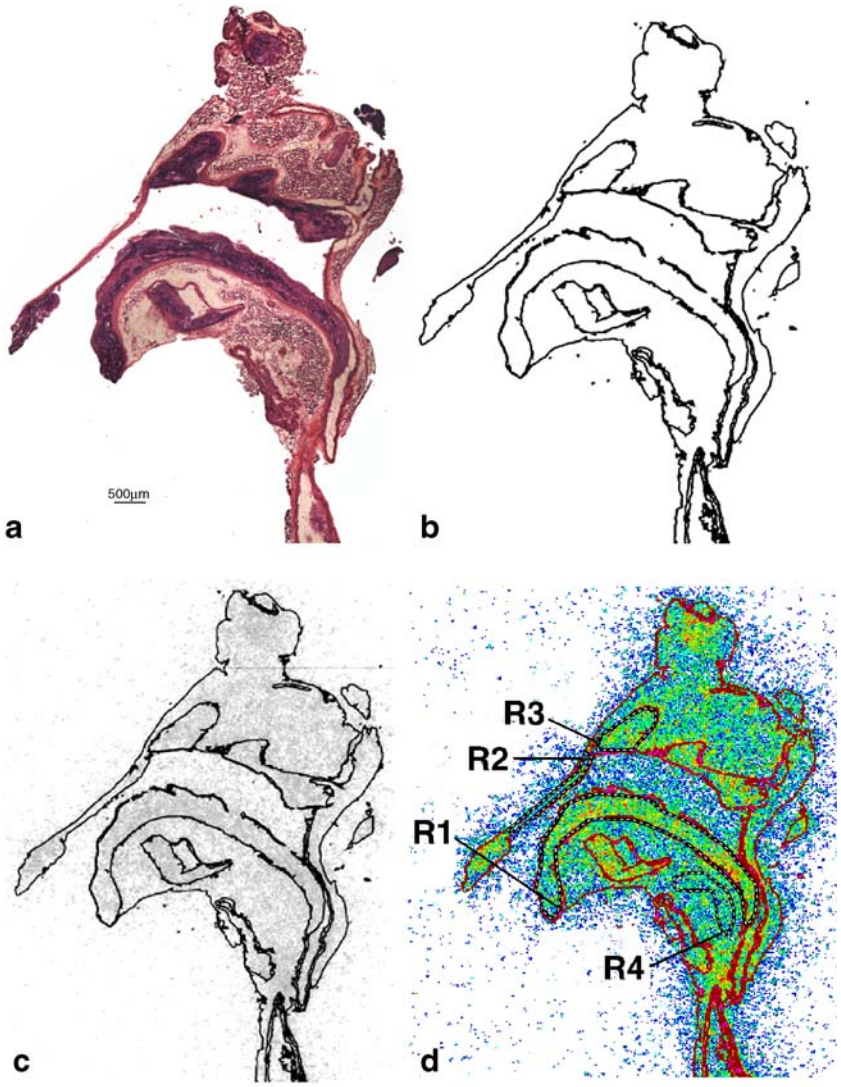

ROI	Area	PSL/mm²	Normalized PSL/mm²
R1+R3 (mean)	Plaque	27.6	4.3
R2	Wall	19.8	3.1
R4	Adventitia	19.0	3.0

e

Fig. 6 An example of analysis of an aortic arch section. **a** HE stain of the section. **b** Patch image made from the HE stained section (**a**). **c** Grey/black autoradiograph superimposed (with ARG picture, not shown) contour image. **d** Rainbow colours of autoradiograph superimposed with contour image and ROI analysis: R1 and R3 = plaque, R2 = healthy vessel wall, R4 = adventitia. In panel **e**, a short example of one aortic arch autoradiography analysis is shown. PSL/mm^2 values are normalized against internal control (muscle) PSL/mm^2 value (data not shown). The calculated single plaque/wall ratio is 1.4 and the plaque/adventitia ratio is 1.5 (the corresponding ratios for the whole study were 1.4 and 1.6)

imaging since both of these integrins are expressed in the intima of atherosclerotic plaques. We do not know whether the integrin $\alpha v\beta 5$ is present in aortic cryosections of the mouse model we used, due to the lack of corresponding anti-mouse antibodies.

^{68}Ga-DOTA-RGD labelling was carried out in high radiochemical purity without any need for further purifications. The labelled compound was found to be quite stable in vivo. A radio-HPLC analysis method was developed in order to separate radioactive degradation products. Little or

no evidence of the dissociation of ^{68}Ga from DOTA within the blood circulation of mice was observed. As anticipated, our ^{68}Ga-DOTA-RGD peptide showed similar in vivo stability in both of the mice strains (LDLR$^{-/-}$ApoB$^{100/100}$ mice and the C57BL/6 J Bom control mice) because the animals were approximately of the same weight and age. ^{68}Ga-DOTA-RGD was cleared from the blood circulation and excreted through the kidneys to the urine with high radioactivity uptake in the intestine, lungs, spleen and liver. We did not find a direct correlation between the uptake of ^{68}Ga-DOTA-RGD and the activity of inflammation in plaques based on the macrophage (Mac-3) staining, indicating that the primary mechanism of uptake is not inflammation.

In the present study, LDLR$^{-/-}$ApoB$^{100/100}$ mouse was used as an animal model of atherosclerosis because this animal shows a high prevalence of atherosclerotic plaques. The lipid profile of this animal resembles the type that is commonly found in human familial hypercholesterolemia and that leads to an accelerated atherogenesis [17, 26]. When fed with a Western-type diet, the LDLR$^{-/-}$ApoB$^{100/100}$ mouse develops arterial lesions with macrophage infiltration and necrotic areas. It is estimated that the developed lesions cover about 15% of the total aortic area [17].

Potential limitations

Since the analysed targets in mouse aorta are small, the analysis is challenging. However, our results concerning the reliability of autoradiography showed very good reproducibility (mean CV% was 4.5%) between analysers. As regards the healthy vessel wall, the CV% was somewhat higher, but still very good (5.8%). This can be expected because of the smaller size of healthy wall and interference from other nearby tissues such as fat.

Despite the significantly increased uptake to atherosclerotic plaques, we were not able to show any difference in the whole-aorta uptake of ^{68}Ga-DOTA-RGD peptide between the LDLR$^{-/-}$ApoB$^{100/100}$ mice and the control mice. This result is partly explained by the other tissue compartments around the healthy vessel wall. In the future, an even more careful removal of the nearby tissue compartments is needed to clarify this issue.

Although we found significantly higher tracer uptakes to plaques, one may speculate on whether the absolute uptake of this tracer to plaques is high enough for in vivo imaging. The plaque/adventitia ratio was 1.6 and the plaque/healthy vessel wall ratio was 1.4, which means that the uptake of ^{68}Ga-labelled DOTA-RGD peptide in this animal model is probably not sufficient for in vivo imaging of atherosclerotic plaques. Obviously, further studies are needed to evaluate the uptake of this tracer in human arterial plaques. The tracer doses used in the present study were high and exceeded radioactivity and peptide doses given to humans, which may have affected the radioactivity uptakes to a certain extent.

Additional substantial improvement in terms of pharmacokinetics is expected to be achieved through the use of multimeric peptides [14]. It is also likely that other agents recognizing the RGD motif, with much higher affinity and/or better selectivity for $\alpha v\beta 3$, may make this approach feasible. Further studies with ^{68}Ga-labelled multimeric RGD peptides and also labelling with other PET isotopes, such as ^{18}F and ^{64}Cu, are warranted. The use of different chelators for ^{68}Ga-labelling, such as 1,4,7-triazacyclononane-1,4,7-triacetic acid (NOTA), may also improve the results. Advantages of ^{68}Ga-NOTA, as compared to ^{68}Ga-DOTA, are higher stability and possibility for labelling in room temperature [21].

Conclusion

Monomeric novel DOTA-RGD peptide was successfully labelled with the generator-produced ^{68}Ga for the imaging of atherosclerotic plaques. The tracer showed reasonably good specific radioactivity and was quite stable in vivo. We observed that the ^{68}Ga-DOTA-RGD uptake in atherosclerotic plaques was significantly increased as compared to the healthy vessel wall. Our findings encourage the pursuit of further studies and testing of different ^{68}Ga-labelled RGD peptides for the imaging of atherosclerotic plaques.

Acknowledgements This study was conducted within the Finnish Centre of Excellence in Molecular Imaging in Cardiovascular and Metabolic Research, supported by the Academy of Finland, University of Turku, Turku University Hospital and Åbo Akademi University. The work was funded by the Finnish Foundation for Cardiovascular Research and Drug Discovery Graduate School of the University of Turku. The authors would like to thank Erja Mäntysalo for excellent assistance in animal experiments, Erica Nyman for performing tissue sectioning and immunostainings, Irina Lisinen for providing expertise in statistical tests, Sanna Hellberg for image processing, and Henri Sipilä for assistance in ^{68}Ga-labelling and HPLC analyses.

Reference

1. Libby P. Inflammation in atherosclerosis. Nature. 2002;420:868–74.
2. Libby P, Theroux P. Pathophysiology of coronary artery disease. Circulation. 2005;111:3481–8.
3. Fan J, Watanabe T. Inflammatory reactions in the pathogenesis of atherosclerosis. J Atheroscler Thromb. 2003;10:63–71.
4. Wintermark M, Jawadi SS, Rapp JH, Tihan T, Tong E, Glidden DV, et al. High-resolution CT imaging of carotid artery atherosclerotic plaques. Am J Neuroradiol. 2008;29:875–82.
5. Waters EA, Wickline SA. Contrast agents for MRI. Basic Res Cardiol. 2008;103:114–21.

6. MacNeill BD, Jang IK, Bouma BE, Iftimia N, Takano M, Yabushita H, et al. Focal and multi-focal plaque macrophage distributions in patients with acute and stable presentations of coronary artery disease. J Am Coll Cardiol. 2004;44:972–9.
7. Schaar JA, Mastik F, Regar E, den Uil CA, Gijsen FJ, Wentzel JJ, et al. Current diagnostic modalities for vulnerable plaque detection. Curr Pharm Des. 2007;13:995–1001.
8. Laitinen I, Marjamäki P, Haaparanta M, Savisto N, Laine VJ, Soini SL, et al. Non-specific binding of [(18)F]FDG to calcifications in atherosclerotic plaques: experimental study of mouse and human arteries. Eur J Nucl Med Mol Imaging. 2006;33:1461–7.
9. Khurana R, Simons M, Martin JF, Zachary IC. Role of angiogenesis in cardiovascular disease: a critical appraisal. Circulation. 2005;112:1813–24.
10. Virmani R, Kolodgie FD, Burke AP, Finn AV, Gold HK, Tulenko TN, et al. Atherosclerotic plaque progression and vulnerability to rupture: angiogenesis as a source of intraplaque hemorrhage. Arterioscler Thromb Vasc Biol. 2005;25:2054–61.
11. Hoshiga M, Alpers CE, Smith LL, Giachelli CM, Schwartz SM. Alpha-v beta-3 integrin expression in normal and atherosclerotic artery. Circ Res. 1995;77:1129–35.
12. Antonov AS, Kolodgie FD, Munn DH, Gerrity RG. Regulation of macrophage foam cell formation by alpha V beta 3 integrin: potential role in human atherosclerosis. Am J Pathol. 2004;165:247–58.
13. Dufourcq P, Louis H, Moreau C, Daret D, Boisseau MR, Lamaziere JMD, et al. Vitronectin expression and interaction with receptors in smooth muscle cells from human atheromatous plaque. Arterioscl Throm Vas. 1998;18:168–76.
14. Beer AJ, Schwaiger M. Imaging of integrin alphavbeta3 expression. Cancer Metastasis Rev. 2008;27:631–44.
15. Burtea C, Laurent S, Murariu O, Rattat D, Toubeau G, Verbruggen A, et al. Molecular imaging of alpha v beta3 integrin expression in atherosclerotic plaques with a mimetic of RGD peptide grafted to Gd-DTPA. Cardiovasc Res. 2008;78:148–57.
16. Indrevoll B, Kindberg GM, Solbakken M, Bjurgert E, Johansen JH, Karlsen H, et al. NC-100717: a versatile RGD peptide scaffold for angiogenesis imaging. Bioorg Med Chem Lett. 2006;16:6190–3.
17. Heinonen SE, Leppänen P, Kholova I, Lumivuori H, Hakkinen SK, Bosch F, et al. Increased atherosclerotic lesion calcification in a novel mouse model combining insulin resistance, hyperglycemia, and hypercholesterolemia. Circ Res. 2007;101:1058–67.
18. Laitinen I, Marjamäki P, Någren K, Laine VJ, Wilson I, Leppänen P, et al. Uptake of inflammatory cell marker [11C]PK11195 into mouse atherosclerotic plaques. Eur J Nucl Med Mol Imaging. 2009;36:73–80.
19. Decristoforo C, Hernandez GI, Carlsen J, Rupprich M, Huisman M, Virgolini I, et al. ^{68}Ga- and 111In-labelled DOTA-RGD peptides for imaging of alphavbeta3 integrin expression. Eur J Nucl Med Mol Imaging. 2008;35:1507–15.
20. Jeong JM, Hong MK, Chang YS, Lee YS, Kim YJ, Cheon GJ, et al. Preparation of a promising angiogenesis PET imaging agent: ^{68}Ga-labeled c(RGDyK)-isothiocyanatobenzyl-1, 4, 7-triazacyclononane-1, 4, 7-triacetic acid and feasibility studies in mice. J Nucl Med. 2008;49:830–6.
21. Li ZB, Chen K, Chen X. (68)Ga-labeled multimeric RGD peptides for microPET imaging of integrin alpha(v)beta (3) expression. Eur J Nucl Med Mol Imaging. 2008;35:1100–8.
22. Horton MA. The alpha v beta 3 integrin "vitronectin receptor". Int J Biochem Cell B. 1997;29:721–5.
23. Hillis GS, Flapan AD. Cell adhesion molecules in cardiovascular disease: a clinical perspective. Heart. 1998;79:429–31.
24. Dijkgraaf I, Kruijtzer JA, Liu S, Soede AC, Oyen WJ, Corstens FH, et al. Improved targeting of the alpha(v)beta (3) integrin by multimerisation of RGD peptides. Eur J Nucl Med Mol Imaging. 2007;34:267–73.
25. Paulhe F, Racaud-Sultan C, Ragab A, Albiges-Rizo C, Chap H, Iberg N, et al. Differential regulation of phosphoinositide metabolism by alpha(V)beta(3) and alpha(V)beta(5) integrins upon smooth muscle cell migration. J Biol Chem. 2001;276:41832–40.
26. Veniant MM, Zlot CH, Walzem RL, Pierotti V, Driscoll R, Dichek D, et al. Lipoprotein clearance mechanisms in LDL receptor-deficient "Apo-B48-only" and "Apo-B100-only" mice. J Clin Invest. 1998;102:1559–68.